Sequence Learning with Passive RFID Sensors for Real-Time Bed-Egress Recognition in Older People

Asanga Wickramasinghe, *Member, IEEE*, Damith C. Ranasinghe, *Member, IEEE*, Christophe Fumeaux, *Senior Member, IEEE*, Keith D. Hill, and Renuka Visvanathan

***Abstract*—Getting out of bed and ambulating without supervision is identified as one of the major causes of patient falls in hospitals and nursing homes. Therefore, increased supervision is proposed as a key strategy toward falls prevention. An emerging generation of batteryless, lightweight, and wearable sensors are creating new possibilities for ambulatory monitoring, where the unobtrusive nature of such sensors makes them particularly adapted for monitoring older people. In this study, we investigate the use of a batteryless radio-frequency identification (RFID) tag response to analyze bed-egress movements. We propose a bed-egress movement detection framework that includes a novel sequence learning classifier with a set of features derived from bed-egress motion analysis. We analyzed data from 14 healthy older people (66–86 years old) who wore a wearable embodiment of a batteryless accelerometer integrated RFID sensor platform loosely attached over their clothes at sternum level, and undertook a series of activities including bed-egress in two clinical room settings. The promising results indicate the efficacy of our batteryless bed-egress monitoring framework.**

***Index Terms*—Batteryless wearable sensor, bed-egress analysis, older people, sequence learning, support vector machines.**

I. Introduction

FALLS in hospitals are common and costly [1]. A U.K. report examining 200,000 incident reports over 12 months found that inpatient falls were the most common (40%) type of safety incident reported [2]. Falls in hospitals were said to be directly responsible for 26 patient deaths, 530 hip fractures, and about 1000 other fractures. In addition to the physical injuries reported, the psychological consequences of falls to the individual include anxiety, depression, loss of confidence, and fear of falling and ultimately a downward spiral of decline in health [3]. Without effective interventions, the overall number and cost of falls in hospitals will increase. Current best practice recommendations contribute to falls prevention in hospitals [4], nevertheless falls rates still remain unacceptably high [5].

In addition to best practices [6], one important approach to reduce falls in hospitals is to increase surveillance opportunities, particularly to minimize patients with high risk of falls getting up from bed without supervision. If alerted in a timely manner, staff are provided with the opportunity to check on patients and offer supervision. More recently, it has been proposed that sensors worn on patients provide better opportunities to simultaneously monitor multiple patients [7]. Movement sensors attached to the body capture biomechanical characteristics of a person's movement [8]–[16]. A number of researchers [8], [12], [16] have used data from movement sensors to recognize activities using empirical classification algorithms where data are processed multiple times introducing unwanted delays to raise an alarm. Response delays have been eliminated in some studies [9], [14] based on machine learning classification techniques, but none has specifically investigated bed-egress recognition. Furthermore, most of these studies [8]–[12], [14], [15] have utilized heavy battery-powered sensors strapped to a patient's body. Additionally, some researchers have considered using multiple sensors in the same platform [8] and sensors attached to different parts of a participant's body [9], [14] to collect rich sets of data for activity recognition. According to studies that evaluate the acceptance of wearable sensors among older people, older people prefer small, lightweight, and low maintenance sensors [17]–[19]. Some people had even refused the use of sensors if using them is complex, e.g., requiring battery maintenance [18]. The obtrusive nature of these sensors can be seen as a hindrance for translation of the technology to practice because older patients regard unobtrusiveness as a key acceptance criteria [20].

Recently, Wolf *et al.* [15] carried out a small (underpowered) clinical trial in a geriatric ward and demonstrated that these kinds of kinematic sensors (body-worn, battery-powered with threshold-based classification techniques) can be used to

Manuscript received December 17, 2015; revised February 29, 2016 and April 30, 2016; accepted May 26, 2016. Date of publication June 2, 2016; date of current version June 29, 2017. This work was supported by in part by a grant from the Hospital Research Foundation (THRF), in part by the Australian Research Council (DP160103039), and in part by the Department of Further Education, Employment, Science and Technology, Government of South Australia.

A. Wickramasinghe and D. C. Ranasinghe are with the School of Computer Science, University of Adelaide, Adelaide 5005, Australia (e-mail: asanga.wickramasinghe@adelaide.edu.au; damith.ranasinghe@adelaide.edu.au).

C. Fumeaux is with the School of Electrical Electronic engineering, University of Adelaide, Adelaide 5005, Australia (e-mail: christophe.fumeaux@adelaide.edu.au).

K. D. Hill is with the School of Physiotherapy, Faculty of Health Sciences, Curtin University, Bentley 6102, Australia (e-mail: keith.hill@curtin.edu.au).

R. Visvanathan is with the Aged and Extended Care Services, The Queen Elizabeth Hospital, Woodville South 5011, Australia (e-mail: renuka.visvanathan@adelaide.edu.au).

Digital Object Identifier 10.1109/JBHI.2016.2576285

recognize bed-egress movements when strapped to the patient's thighs with bandages. Unfortunately no quantitative data were provided regarding the performance of the sensor system.

In contrast, we demonstrated in [16], for the first time, the possibility of using batteryless, and therefore, lightweight radio frequency identification (RFID) technology with integrated kinematic sensors as a bed-egress movement sensor alarm in young healthy participants. Unlike methods employed in previous studies [8], [12], [15], where the sensor was strapped to a patient, we considered a more comfortable attachment method where the sensor was more likely to be acceptable by older people [21]. In our approach, the sensor was attached to a loosely worn garment over the sternum. The algorithm reported in [16] relies on thresholds applied to a 20-s data stream segment after interpolation and filtering to, first, determine a posture transition based on sit-to-stand motion analysis used in [8], and subsequently, identify a bed-egress movement. Consequently, this approach can result in delays of up to 20 s to generate notifications to caregivers from the time of an actual bed-egress; thus increasing the time to respond to a bed-egress. Subsequently, in [21], we employed a machine-learning-based activity classifier (conditional random fields—CRF) to classify segments of sensor observations and achieved better performance compared to the empirical algorithm in [16], but real-time inferencing was not supported.

In this paper, we propose a monitoring framework that combines a novel sequence learning algorithm suitable for sparse accelerometer and RFID data. The framework is capable of generating a bed-egress alarm in real time (see Section II). Our approach is based on a wearable embodiment of a triaxial accelerometer integrated in a passive RFID platform, which is loosely attached over a garment at the sternum level. In particular:

1) We propose a bed-egress monitoring framework (see Section II-C) based on a novel sequence learning algorithm that utilizes accelerometer and RFID data while exploiting only time-domain features to support rapid feature calculations. The algorithm is suitable for sparse data streams, a characteristic of passive sensor enabled RFID tags (see Section II-D). The sequence learning algorithm considers recent past sensor observations and their activity labels to model the sequential nature present in sparse data streams.
2) Based on bed-egress motion analysis, we developed nine types of new features relying only on time-domain information from acceleration signals and the strength of a received RFID tag signal (see Section II-E). Furthermore, we propose four types of features to capture the sequential nature of bed-egress motion from recent activity label history (see Section II-F).
3) We have evaluated the *alarming performance* of our approach in community dwelling older people (66–80 years) (see Section II-B). Since powering and gathering observations from the sensor is dependent on hardware (antennas) configuration (see Section II-A), and we are interested in reducing falls in hospitals, we have studied the performance of the sensor in two deployment settings suitable for hospital rooms in geriatric wards.

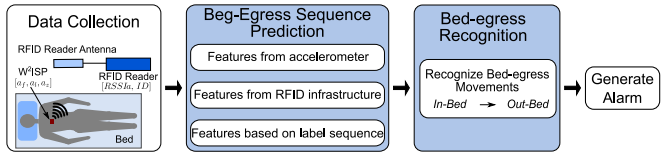

Fig. 1. Illustration of bed-egress movement analysis framework.

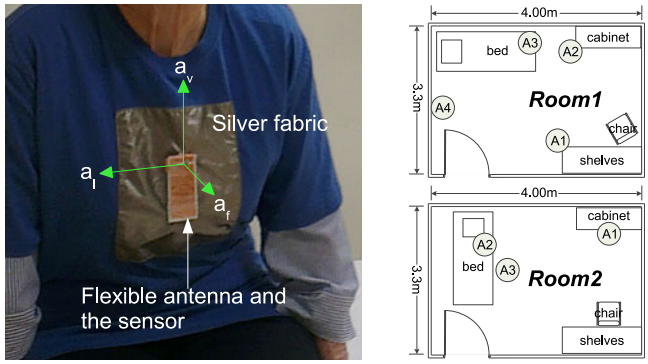

Fig. 2. (a) Older person wearing the W²ISP sensor (≈ 3 g, size 18 × 20 × 2 mm), flexible antenna (36 × 85 × 2 mm) and isolating silver fabric (230 × 220 mm); (b) *RoomSet1* and *RoomSet2* room and equipment configuration. All ceiling antennas (A3 in *RoomSet1* and A2 and A3 in *RoomSet2*) were inclined toward middle section of the bed.

II. Methods

Fig. 1 illustrates our proposed framework to recognize bed-egress movements. We describe our proposed framework in detail in the following sections.

A. RFID Sensor Platform

The RFID sensor platform used in this study consists of: 1) a passive sensor enabled RFID tag called wearable wireless identification and sensing platform (W²ISP), which is based on the WISP in [22] [see Fig. 2(a)]; and 2) RFID infrastructure consisting of a commercial-off-the-shelf UHF RFID reader (Impinj IPJ-REV-R420-GX11M operating in the frequency range 920–926 MHz) and circularly polarized antennas (Laird S9028PCLJ) [23]. The W²ISP contains a triaxial accelerometer (ADXL330) with a flexible antenna for wearability [24]. The W²ISP is small, lightweight, inexpensive, and battery free. The W²ISP works on the energy collected from the electromagnetic field illuminating it [23]. The RFID infrastructure is used to energize and collect data from the W²ISP where the communication is governed by the air interface protocol ISO 18000-6C [25], [26]. A single RFID sensor platform can communicate with multiple W²ISPs and individual W²ISP tags can be identified using the unique electronic identifier communicated by the W²ISP along with the sensor data.

There are two information sources available from this setup (see Fig. 1). First, the triaxial accelerometer embedded in W²ISP measures the acceleration resulting from a participant's motion and the component of gravity along the accelerometer's axes: frontal (a_f), vertical (a_v), and lateral (a_l). Second, the RFID reader provides tag activation and measures the strength of the wireless signal backscattered from the W²ISP tag, where this

information is correlated with the distance between an RFID reader antenna and the W^{2}ISP (see Appendix A). The signal strength received at a particular RFID reader antenna is referred to as the received signal strength indicator (RSSI) [23] and it is recorded with the antenna identifier (aID) that captured a given reading from the W^{2}ISP. Thus, a single sensor observation can be represented as the five tuple $[a_f, a_v, a_l, \text{RSSI}, a\text{ID}]$.

B. Data Collection

The study protocol (protocol number 2011129) was reviewed and approved by Human Research Ethics Committee of The Queen Elizabeth Hospital, South Australia. We conducted a pilot study with 14 healthy older volunteers (four male and ten female participants) aged between 66 and 86 years. For this study, the participants had to be 65 years or older, living at home, able to consent to the study and mobilize independently. The participants were recruited from geriatrician clinics and from volunteer lists from other studies. First, potential participants were contacted over the phone, and then, participation information sheets were mailed. During the trial informed consent was obtained from the participants and no honorarium was paid. Fourteen participants responded and volunteered to participate in the study and the study was completed over a two-month period.

From our preliminary experiments, we identified that it requires at least three RFID reader antennas to adequately illuminate the room. Therefore, data collection was carried out in two different clinical room settings [*RoomSet1* and *RoomSet2* illustrated in Fig. 2(b)] that differed in layout, antenna placement and number of antennas deployed. Our room settings were designed to investigate a general hardware deployment option (i.e., antenna placement) suitable for hospital ward rooms furnished with a bed and an armchair. *RoomSet1* antenna deployment was designed to illuminate the whole room. In contrast, *RoomSet2* deployment was designed to only illuminate areas where patients were most likely to spend the most amount of time. In both room configurations, RFID antennas are placed above the level of the bed and at or near ceiling height to reduce possible obstructions of interrogation signals from RFID reader antennas and responses from the W^{2}ISP. Data collected from *RoomSet1* and *RoomSet2* configurations are simply referred as *RoomSet1* and *RoomSet2*, respectively. In terms of the RFID infrastructure cost, *RoomSet1* configuration is more costly compared to *RoomSet2* because *RoomSet1* has one additional antenna.

During the trial, participants were informed what types of activities they were required to perform and the worn sensor was used to capture the motion resulting from these activities. Participants performed activities that included: 1) lying on the bed; 2) sitting on the bed; 3) getting out of the bed; 4) sitting on the chair; 5) getting out of the chair; and 6) going from *A* to *B* (*A* and *B* represent the bed, chair or door). Each participant performed activities on two broadly scripted activity lists. No particular order was used for selecting the scripts and the number of scripted routines, and no instructions on how to perform activities were given to the participants. A researcher who was present during the trial labelled the sensor data using an annotating software developed to record sensor data. A trial with each volunteer lasted between 60 and 90 minutes. One participant contributed to both datasets. Due to a faulty antenna contact of our sensor prototype, the data from the common participant for *RoomSet1* was not usable and hence removed from the analysis.

TABLE I
DATASET STATISTICS

Configuration	*RoomSet1*	*RoomSet2*
Mean intersensor observation time difference (seconds)	0.36 (2.43)	0.79 (9.62)
Mean intersensor observation time difference using data up to the 95th percentile (s)	0.20 (0.26)	0.31 (0.26)
Length of data per participant (s)	2116 (1006)	3596 (268)
# of in-bed samples	45922	21782
# of out-bed samples	6335	864

Corresponding standard deviation values presented within parenthesis.

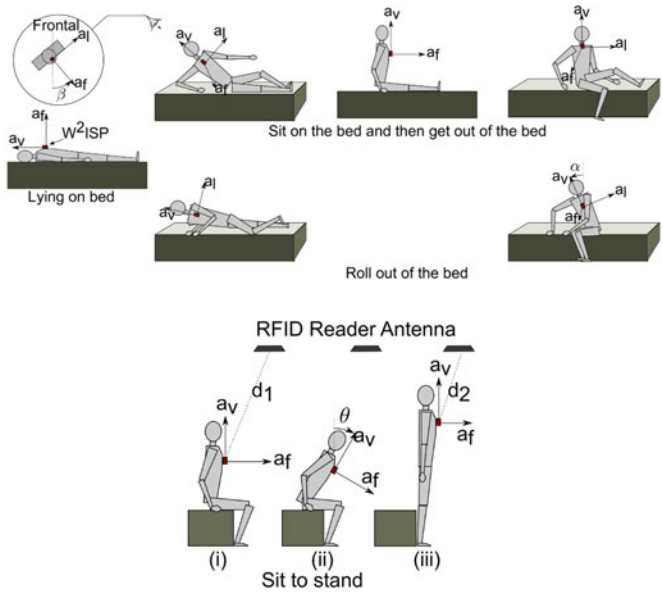

Fig. 3. Analysis of ambulating out of lying posture.

Table I presents statistics of the collected datasets. It is important to note that the majority of the samples from both datasets were collected when the participants are *in-bed*. Although there are 14 participants in these datasets, the amount of data collected is sufficiently large and the distribution of data across *in-bed* and *out-bed* is similar to a real-world deployment setting where patients are most likely to spend time in their beds. These datasets are publicly available at the project website.[1]

C. Bed-Egress Monitoring Framework

Human motion analysis of a participant (see Fig. 3) provides the basis for formulating the bed-egress monitoring framework. Bed-egress activity involves a sequence of movements (see Fig. 3) that are reflected in the sensor observations (see Fig. 4). In this movement sequence, we are interested in transitions from

[1]Project website: http://autoidlab.cs.adelaide.edu.au/research/ahr

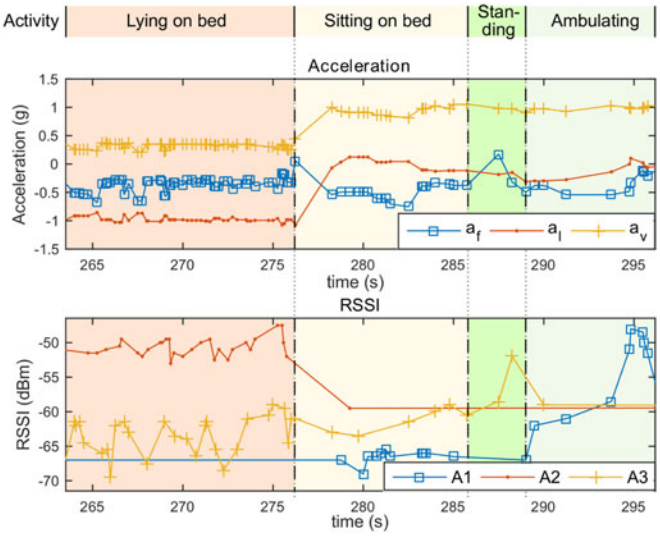

Fig. 4. Acceleration and RSSI signal patterns collected from W^{2}ISP for *RoomSet2* when a participant got out of the bed from lying on bed (lying on side). This also indicates the sparsity (variable intersensor observation time differences) of the sensor data streams.

in-bed to *out-bed*. Therefore, we formulate bed-egress recognition as follows:

First predicting activity label sequence, *in-bed* or *out-bed*, in real time for a sequence of sensor observations;

Then determining changes from *in-bed* to *out-bed* in the predicted activity label sequence to recognize bed-egress movements.

Here, we have considered the entire bed-egress motion including possible variations observed to capture the contextual information of a bed-egress (see Section II-E). The remaining sections of the paper discuss the proposed framework in detail.

D. Bed-Egress Sequence Prediction

Researchers have looked at stochastic modeling of RFID data streams using techniques such as particle filters [27] and partially observable Markov decision process [28] to address the uncertainty in RFID tag observations mainly due to the random access nature of ISO 18000-6C protocol [25]. In contrast to our goal, that is assigning a class label to each sensor observation from W^{2}ISP, their goal is to track RFID tags, i.e. , to ascertain the location of a given tag at a given point in time when it cannot be observed by an RFID infrastructure.

Prediction of a sequence of activity labels (*in-bed* or *out-bed*) from a sensor observation sequence can be modeled as a sequence learning problem. Regular sequence learning algorithms, such as linear chain CRF learns relationships between ith and $(i+1)$th elements in a sequence; in other words, these algorithms model a sequence as a first-order Markov chain [29]. As shown in Fig. 4, the sensor data stream obtained from a W^{2}ISP has variable intersensor observation time differences. Therefore, regular sequential learning algorithms' reliance on a single previous sensor observation (which might belong to an activity in the distant past) may result in poor bed-egress movement recognition performance. To this end, we follow the deterministic approach proposed for sequential learning in [30] and propose the following sequence learning algorithm suitable for sparse data streams based on the support vector machine (SVM) classifier. As opposed to considering a fixed number of elements in a sequence, we considered elements in a fixed time interval to model the sequential relationship; this approach mitigates past observations that belong to an activity in the distant past from adversely affecting the prediction of the current activity. In the following, we describe the two main steps of the algorithm, i.e. , inferencing and training.

1) Representation and Inference: We denote the ith sensor data at time t_i, $t_i > t_{i-1}$, $i \in \mathbb{N}$, using the pair (t_i, s_i), where $s_i = [a_f, a_v, a_l, RSSI, aID]$. Because of the irregular nature of the data collection, the sequence of collected data $X = \{(t_i, s_i)\}_{i\geq 1}$, $i \in \mathbb{N}$ is a nonuniform time series. We denote the corresponding sequence of activities for each sensor observation using $Y = \{y_i\}_{i\geq 1}, y_i \in C$, where C is the possible set of class labels; in this study we consider only two class labels, $C = \{in\text{-}bed, out\text{-}bed\}$. We use subscripts to denote subsequences; for instance $X_{[a,b]}$ denotes the sensor data stream segment for time interval $[a, b]$, where $b > a$. The notation $\langle \cdot, \cdot \rangle$ is used to represent the vector inner product.

In our research, given a sensor observation sequence, $X = \{(t_i, s_i)\}_{i=0}^{m}$, the inference procedure assigns the class label, y_i to each corresponding sensor observation, (t_i, s_i) considering correlations between most recent sensor observations and labels for a fixed duration of δt; i.e., considering $Y_{[t_i-\delta t, t_i]}$ and $X_{[t_i-\delta t, t_i]}$. Since we are interested in real-time prediction, we specifically focus on the greedy inference procedure discussed in [30]. To this end, we assume that the predictions already made are frozen and there exist a score function that calculate a score for assigning the class label y for the ith sensor observation

$$S_i(w, X, Y, y) = \langle w, \phi(X_{[t_i-\delta t, t_i]}, Y_{[t_i-\delta t, t_{i-1}]}, y)\rangle \quad (1)$$

where $w \in \mathbb{R}^d$ is a learned model also known as parameter vector and $\phi : X_{[a,b]} \times Y_{[a,b]} \times y \mapsto \mathbb{R}^d$ is called the feature mapping function that captures the sequential information in a single feature vector.

The inference procedure determines successive class labels, y_i, based on maximizing the score function in (1); i.e., $\arg\max_{y\in C} S_i(w, X, Y, y)$. In fact, as we have frozen the previous predictions, the prediction function can be represented as a recursive function

$$f_i(w, X) = \text{argmax}_{y\in C} \langle w, \phi(X_{[t_i-\delta t, t_i]}, f_{[t_i-\delta t, t_{i-1}]}(w, X), y)\rangle. \quad (2)$$

where $f_{[a,b]}(w, X)$ represents the predictions from time a to time b.

The feature function, ϕ, in our bed-egress sequence prediction algorithm is significant as it essentially captures patterns in the data stream. We specifically considered a feature function of the form $\phi(X_{[t_i-\delta t, t_i]}, Y_{[t_i-\delta t, t_{i-1}]}, y) = [\phi_I(X_{[t_i-\delta t, t_i]}, y), \phi_P(Y_{[t_i-\delta t, t_{i-1}]}, y)]$, where ϕ_I calculates features based on the considered class label, y, with observed information $X_{[t_i-\delta t, t_i]}$ (see Section II-E), and ϕ_P considers the

label sequence $Y_{[t_i-\delta t,t_{i-1}]}$ and y (see Section II-F) to calculate features.

2) Training: The goal of the classier training is to find the model w that minimize the classification error. According to the prediction function (2), we can observe that the score for a given sensor observation with the correct class label $S_i(X,Y,y_i)$ must be greater than the score of all other class labels $S_i(X,Y,y), y \in C \setminus y_i$, i.e., $S_i(X,Y,y_i) > S_i(X,Y,y)$. In SVM setting, $S_i(X,Y,y_i)$ should be at least greater than a margin, which is typically set to 1 [31]. Consequently, the updated constraint for minimizing the error for the SVM training is $S_i(X,Y,y_i) \geq S_i(X,Y,y) + 1$.

Notably, as indicated by the nature of the feature function, two instances of output vectors from the feature function, $\phi(X_{[t_i-\delta t,t_i]}, Y_{[t_i-\delta t,t_{i-1}]}, y)$ and $\phi(X_{[t_j-\delta t,t_j]}, Y_{[t_j-\delta t,t_{j-1}]}, y)$, where $i \neq j$, can be considered independent of each other. This characteristic enables formulating efficient learning algorithms as described in [30]. In this setting, labeled sensor data stream segments from multiple sequences can be considered for learning, unlike in other sequence learning algorithms.

The primal form of soft margin SVM formulation for the proposed sequence learning algorithm followed the formulation of soft margin SVM presented in the work entitled "large margin methods for structured and interdependent output variables" [31]. Specifically, we utilized the slack rescaling method in [31] to incorporate different costs for misclassifications. The classification model, w, is learned by minimizing the following constrained convex objective function (3):

$$\begin{aligned} \min_{w,\xi_i} \quad & \frac{\lambda}{2}\|w\|^2 + \frac{1}{M}\sum_{i=1}^{M}\xi_i \\ \text{subject to} \quad & \forall i \ \langle w, \phi_i(y_i)\rangle - \langle w, \phi_i(y_r)\rangle \geq 1 - \frac{\xi_i}{\Delta(y_i,y_r)} \\ & \forall i \ \xi_i \geq 0 \\ \text{where} \quad & \phi_i(y) = \phi(X_{[t_i-\delta t,t_i]}, Y_{[t_i-\delta t,t_{i-1}]}, y) \\ & y_r = \arg\max_{y \in C\setminus y_i} \langle w, \phi_i(y)\rangle. \end{aligned} \tag{3}$$

Here, M is the length of the training dataset, λ is the regularization parameter that is treated as a model parameter, and $\Delta(y_i,y_r)$ is a cost function that assigns different costs based on the nature of misclassifications. Any margin violations are treated as positive errors that are represented by ξ_i; as a result, value of the objective function is increased that subsequently updates the classification model to reduce the objective value.

In this study, we consider a cost function of the following form:

$$\Delta(y_i,y_r) = \begin{cases} 1 & ; \text{if } y_i = \text{in-bed} \wedge y_r = \text{out-bed} \\ c & ; \text{otherwise} \end{cases} \tag{4}$$

where c is the relative cost of misclassifying an *out-bed* instance as *in-bed* and c is also considered as a model parameter.

We use the Pegasos algorithm [32] to solve the optimization problem in (3) directly using its primal form. Unlike other methods such as LaRank [30], which optimizes SVMs in dual form, optimizing in primal form is attractive where there are a large number of training samples as in our case. When using the Pegasos algorithm two additional parameters need to be specified; 1) number of iterations, T and 2) minibatch size, k. In total, the proposed bed-egress sequence prediction algorithm requires four model parameters, i.e. , λ, c, T, and k, and they are selected using cross validation as described in Section II-G. We have made the implemented algorithm publicly available at the project website.[1]

E. Features Based on the Sensor Observation Sequence

As illustrated in Fig. 3, participants may lift their trunk to a vertical position using their dominant arm when they are lying in supine posture and then turn their body facing the edge of the bed to place their legs on the ground. Furthermore, they can roll over to the edge of the bed, and then, use the weight of their legs and arm to raise their trunk to a vertical position. When sit-to-stand posture transition is considered, as also shown by Najafi *et al.* [8], participants first bent forward (stage (ii) in sit to stand transition in Fig. 3) and then stand up.

As discussed in Section II-A, we have two information sources in our data stream. Considering a segment of sensor observations for the *i*th sensor observation, $X_{[t_i-\delta t,t_i]}$, we extracted the features described in the following. Detailed formulas are provided in Appendix B. From our preliminary experiments, we identified approximately 2 s are required for a person to get out of the bed while being seated. Therefore, we set $\delta t = 2\,s$ to calculate these features.

1) Features from the Acceleration Sensor: As the W^{2}ISP data stream is a nonuniform time series, a faithful calculation of frequency-domain features, as in [8], [9], and[14], without preprocessing is not possible [33]. Hence, we focus on time-domain features [8]–[11], [14] and features based on biomechanics [8], [12], [34] by analyzing bed-egress motion illustrated in Fig. 3 to avoid unwanted delays in real-time prediction. These extracted features are presented in Table II.

We obtained nine features using the *i*th sensor observation ($\{1,\ldots,9\}$ in Table II). During the sit-to-stand transition, the acceleration in the vertical direction a_v and the trunk rotational motion on the sagittal plane (θ) [8] provide a good description of the motion. Furthermore, as shown in Fig. 3, rotational motion of the trunk on coronal (α) and transverse (β) planes also provide information on the bed-egress motion of a participant apart from the directly measured acceleration signal. To capture these patterns, we utilized acceleration signals (a_f, a_l, and a_v) and approximated trunk rotational motion on sagittal (θ), coronal (α), and transverse (β) planes ($\{1,\ldots,6\}$ in Table II). Based on angles (θ, α, and β), we also estimate the acceleration signals relative to the human body ($\{7,8,9\}$ in Table II) on anteroposterior axis (a_x), mediolateral axis (a_y), and dorsoventral axis (a_z) (see Appendix B-A).

We extracted 37 further features based on a sensor data stream segment $X_{[t_i-\delta t,t_i]}$. We extract common time-domain features, namely mean, maximum, minimum values for the three acceleration signals (a_f, a_l, and a_v) and the approximated angles (θ,

TABLE II
FEATURES FROM ACCELERATION SIGNALS

Feature #	Feature
1	a_f—Frontal acceleration
2	a_l—Lateral acceleration
3	a_v—Vertical acceleration
4	θ—$\measuredangle$ on Sagittal plane [8], [12], [16], [34]
5	α—$\measuredangle$ on Coronal plane
6	β—$\measuredangle$ on Transverse plane
7	a_x—Anteroposterior acceleration (using θ, a_f, and a_v)
8	a_y—Mediolateral acceleration (using α, a_l, and a_v)
9	a_z—Dorsoventral acceleration (using θ, α, a_f, a_l, and a_v)
10, 11, 12	mean(a_f), mean(a_l), mean(a_v) [9], [34], [35]
13, 14,15	max(a_f), max(a_l), max(a_v) [35]
16, 17, 18*	min(a_f), min(a_l), min(a_v)
19, 20, 21*	$t_{\max(a_f)} < t_{\min(a_f)}, t_{\max(a_l)} < t_{\min(a_l)}, t_{\max(a_v)} < t_{\min(a_v)}$
22, 23, 24	corr(a_f, a_l), corr(a_f, a_v), corr(a_l, a_v) [9]
25, 26, 27	mean(a_x), mean(a_y), mean(a_z)
28, 29, 30	Δv_x, Δv_y, Δv_z [8]
31, 32, 33	Δd_x, Δd_y, Δd_z [8]
34,	Δv_r [12]
35, 36, 37	mean(θ), mean(α), mean(β)
38, 39, 40*	max(θ), max(α), max(β)
41, 42, 43*	min(θ), min(α), min(β)
44, 45, 46*	$t_{\max(\theta)} < t_{\min(\theta)}, t_{\max(\alpha)} < t_{\min(\alpha)}, t_{\max(\beta)} < t_{\min(\beta)}$

*Newly engineered features.

TABLE III
FEATURES FROM RFID PLATFORM

Feature #	Feature
1	mean(RSSI$_a$), $a \in \mathcal{A}$ [36]
2	max(RSSI$_a$), $a \in \mathcal{A}$ [36]
3	min(RSSI$_a$), $a \in \mathcal{A}$ [36]
4*†	mean(RSSI$_{a_j}$) $a \in \mathcal{A}, j = 1 \cdots 3$
5*†	mean(RSSI$_{a_j}$) > mean(RSSI$_{a_{j+1}}$) $a \in \mathcal{A}, j = 1, 2$
6	ant$_a$ = $\mathbf{1}_{[a \in S_i(a\text{ID})]}$, $a \in \mathcal{A}$ [34]
7	MI2 $\in \mathbb{R}^{\lvert\mathcal{A}\rvert}$ [34]
8*	$miC \in \mathbb{R}^d$, $d = {}_{\lvert\mathcal{A}\rvert}C_2$

* Newly engineered features.
† RSSI$_{a_j}$: RSSI values received for antenna a for the subsegment $\mathfrak{S}_j$.

α, and β) ($\{10 \dots 18\}$ and $\{35 \dots 43\}$ in Table II). Although researchers in [35] have considered the maximum value of acceleration signals, minimum value has been overlooked. Both maximum and minimum values provide extreme values that indicate posture transitions similar to that described in [8]. We also considered the temporal location of the maximum value with respect to the minimum value for each acceleration axis and each angle ($\{19, 20, 21\}$ and $\{44, 45, 46\}$ in Table II) as they are indicative of posture transitions as observed in Fig. 3. The features Δv and Δd denote the approximated change in velocities and displacements for a given sensor data segment in Table II $\{28 \cdots 34\}$ (see Appendix B-A). Although researchers in [8] and [12] have considered difference in velocity and displacement along the vertical axis, we have considered all three axes as bed-egress motion depicts movements in all the axes. Additionally, resultant velocity Δv_r [12] is also considered as a feature.

2) Features from the RFID Infrastructure: It is noteworthy that the distance between the sensor and a fixed RFID antenna also varies as a result of human motion. This change in distance is reflected in the RSSI measured by the RFID platform as RSSI is hypersensitive to the distance, d, between an antenna and the tag; i.e., RSSI $\propto 1/d^4$ [23] (see Appendix A). For instance, during the sit-to-stand transition illustrated in Fig. 3, the distance from the W^{2}ISP to the RFID antenna while the participant is sitting on the bed (d_1) is greater than the distance from the W^{2}ISP to the RFID antenna while the participant is standing (d_2), i.e. $d_1 > d_2$. In Fig. 4, we can see a lower RSSI value for A3 when a participant is sitting on the bed compared to when the participant is standing because of the larger distance between the W^{2}ISP and A3. Similarly, we can see that when the participant is ambulating, in this case toward the chair, the RSSI for A1 is also increased, mainly due to the decrease in distance between the W^{2}ISP and A1. Features extracted based on information from the RFID infrastructure, presented in Table III, capture the aforementioned patterns. Here, we denote the set of antennas used to collect data as $\mathcal{A}$ and the set of RSSI values for a given antenna $a \in \mathcal{A}$ as RSSI$_a$.

We calculated time-domain features, mean, maximum, and minimum value of the RSSI for a segment ($\{1, 2, 3\}$ in Table III) to capture these patterns. Time-domain features from RSSI have also been used recently for activity recognition in [36]. However, they were applied to a deployment where both RFID antennas and RFID tags were attached to the participant's body.

Relative RSSI differences are less variable with respect to each participant. Therefore, to capture patterns using relative RSSI, we considered a $3\delta t = 6$ s segment, $X_{[t_i - 3\delta t, t_i]}$, equally subdivided in time into three equal subsegments ($\mathfrak{S}_j = X_{[t_i - j\delta t, t_i - (j-1)\delta t]}, j = 1 \dots 3$). Using these subsegments, we extracted mean RSSI values and features comparing the relative magnitudes of subsegments ($\{4, 5\}$ in Table III).

As shown in Fig. 4, the RFID reader antennas that collect sensor observations vary with the location of the participant because to the RFID antenna facing the sensor is most likely to power and collect the response from the W^{2}ISP. We capture this using a binary feature, ant $\in \{0, 1\}^{\lvert\mathcal{A}\rvert}$ ($\{6\}$ in Table III).

Researchers in [34] utilized a mutual information (MI)-based feature to capture the correlation between antennas for a given segment. Given a sensor observation sequence, they obtained an MI matrix, M, for every pair of antennas as follows:

$$m_{\mathrm{aa}'} = \frac{1}{n} \sum_{i=1}^{n-1} \mathbf{1}_{[\{a, a'\} = \{a_i, a_{i+1}\}]}. \tag{5}$$

Here, an element $m_{\mathrm{aa}'}$ in M represents the weighted number of cooccurrences of observations from antenna a and antenna a', $\mathbf{1}_{[x]}$ assumes 1 if x is true and 0 otherwise, and a_i is the antenna ID for the ith sensor observation. We use the $MI2$ approach described in [34] as one of the features ($\{7\}$ in Table III). Furthermore, in this study, we calculated a novel feature, referred as *antenna cooccurrences* (*miC*) ($\{8\}$ in Table III), by obtaining an MI matrix per segment $X_{[t_i - 2, t_i]}$ and considering the combinations of different antennas, ${}_{\lvert\mathcal{A}\rvert}C_2$ as features (see Appendix B-B).

TABLE IV
FEATURES FROM LABEL SEQUENCE

Feature #	Feature
1	$\phi_{p1} \in R^{3\|C\|}$—Relationship between y and 3 previous class labels
2	$\phi_{p2} \in R^{\|C\|}$—Time weighted label count
3	$\phi_{p3} \in R^{d'}$, $d' = {}_{\|C\|}P_2$—Number of changes in activity labels
4	$\phi_{p4} \in R^{\|C\|}$—Last activity transition time relative to $t_i - \delta t$

F. Features Based on a Label Sequence

These features are designed specifically to capture the transition of activities during a bed-egress motion. We specifically considered four features (ϕ_{pj}, $j = \{1 \ldots 4\}$) from previous labels $Y_{[t_i - \delta t, t_{(i-1)}]}$ and the current class label y (see Table IV). We have selected $\delta t = 2 \times 4 = 8$ s to obtain sufficient information relating to transition of activities as we have identified that a participant took approximately 2 s to get out of the bed while seated during our preliminarily experiments.

Relationships between y and three previous class labels were considered as features, $\phi_{p1} \in R^{3|C|}$. Here, we partition the output vector from ϕ_{p1} into two partitions, and depending on y, previous three class labels are assigned to corresponding partitions (see Appendix B-C).

Time-weighted count of labels is also used as a feature ($\phi_{p2} \in R^{|C|}$). Here, we assigned the highest weight to the class label at time t_i and the weights were decreased linearly to 0 at time $t_i - \delta t$. Weight at time t, $t_i - \delta t \leq t \leq t_i$, is given by $\tau_t = (t - t_i + \delta t)/\delta t^2$ such that $\int_{t_i - \delta t}^{t_i} \tau_t = 1$. Using this approach, emphasis is given to the recent class labels with respect to the ith observation.

Given a sufficiently small time period δt, typically, participants do not transition between activities more than once, i.e., they do not get out from and get into a bed in quick succession. Therefore, we consider the number of changes in activity labels as a feature (ϕ_{p3}). As there are two classes in our setting, i.e., *in-bed* and *out-bed*, this feature can be represented by $\phi_{p3} \in R^{d'}$ where $d' = {}_{|C|}P_2$.

We also considered the time that the last activity transition is observed ($\phi_{p4} \in R^{|C|}$). This time is considered relative to $t_i - \delta t$. Based on the transition, i.e., *in-bed to out-bed* or *out-bed to in-bed*, the transition time is assigned to the corresponding position of the output vector from ϕ_{p4}.

G. Statistical Analysis

The overarching goal of the bed-egress motion analysis framework is to recognize the most number of bed-egress movements with less false recognitions as much as possible to avoid alarm fatigue. It is important to exercise immediate interventions, while eliminating false bed-egress recognitions; therefore, we also evaluate bed-egress movement recognition in terms of latency.

In order to evaluate bed-egress recognition performance, we defined a true positive (TP) as a bed-egress movement recognized 5 s prior to the participant was known to be *out-bed* or when the participant was known to be *out-bed* (i.e., they are already out of bed). All other bed-egress movements while the participant was *in-bed* were incorrect, and hence, counted as false positives (FPs). The missed bed-egress movements are treated as false negatives (FNs). We evaluated bed-egresses after a δt duration from the start of a trial to provide sufficient information to our inference algorithm. We present precision (positive predictive value) and recall (true positive rate) of bed-egress movements along with the values of TPs, FPs and actual number of bed-egress movements [37]. We calculate precision as $P = TP/(TP + FP)$. Precision measures the number of false positives with respect to all bed-egresses detected by our approach and higher precision is associated with lower false bed-egress detections in our setting. Recall is calculated as $R = TP/(TP + FN)$. It measures the detection of true bed-egress movements relative to actual bed-egress movements in the data stream, consequently, higher recall indicates a lower number of misses.

In order to evaluate the latency, we considered the time taken from the actual bed-egress movement (i.e., based on the ground truth) to the predicted bed-egress movement as the delay. Delays for bed-egress movements that are predicted prior to the actual bed-egress movement are taken as zero.

Parameter selection for the sequence learning classifier is performed using G-mean = sqrt(sensitivity × specificity), which is the geometric mean of recall (sensitivity) and specificity (true negative rate) that are obtained using the standard confusion matrix for binary classification [38]. Since bed-egress movements are determined as changes from *in-bed* to *out-bed*, optimizing the sequence learning classifier on sensitivity increases the bed-egress recognition performance.

We used leave-one-patient-out cross validation to evaluate the performance of our framework. Denoted a set of data collected from participant i as $\mathcal{D}_i$, the whole dataset is defined as $\mathcal{D} = \cup_{i=1}^{n} \mathcal{D}_i$, where n is the number of participants in the dataset. Given a participant, p, $\mathcal{D}$ is partitioned into three subsets: 1) $\mathcal{D}_p \in \mathcal{D}$—test set; 2) $\mathcal{D}_j \in \mathcal{D} \setminus \mathcal{D}_p$—validation set; and 3) $\mathcal{D}_j \in \mathcal{D} \setminus (\mathcal{D}_p \cup \mathcal{D}_j)$—training set, where j is a randomly selected participant. We train the classifier using the training sets and obtained the G-mean by evaluating the trained models using the corresponding validation sets to select a set of model parameters that maximizes the mean G-mean measure. Finally, we present the results obtained using the test set $\mathcal{D}_p$, using classifier trained using $\mathcal{D} \setminus \mathcal{D}_p$ based on the selected set of model parameters. This evaluation scheme is close to practical usage of the framework because initially training is carried out using data collected by a subset from the target population, and then, the trained model is to recognize bed-egress movements of the other participants who are unknown to the learned model.

III. RESULTS

A. Bed-egress movement recognition

Table V shows the bed-egress movement recognition results for TPs, FPs, precision, and recall for *RoomSet1* and *RoomSet2* using the proposed framework and our previously published approach, Bed Exit Alert System (BEAS) [21] for comparison. Since we need real-time predictions, for BEAS, we used the

TABLE V
BED-EGRESS RECOGNITION PERFORMANCE (ALARMING PERFORMANCE)

			Proposed Framework				BEAS Proposed in [21]			
Participant	Gender	Actual	TP	FP	Precision	Recall	TP	FP	Precision	Recall
RoomSet1 ($T:1000, k:100, \lambda:10^{-8}, c:0.7$)*										
1	M	11	5	0	100.0	45.5	5	39	11.4	45.5
2	F	7	4	2	66.7	57.1	7	14	33.3	100.0
3	F	9	4	1	80.0	44.4	4	6	40.0	44.4
4	F	4	4	0	100.0	100.0	4	2	66.7	100.0
5	F	6	6	0	100.0	100.0	5	7	41.7	83.3
6	F	14	6	1	85.7	42.9	6	78	7.1	42.9
7	M	10	5	1	83.3	50.0	8	48	14.3	80.0
8	M	7	1	1	50.0	14.3	3	116	2.5	42.9
9	F	14	5	1	83.3	35.7	9	14	39.1	64.3
Total		82	40	7	**85.1**	48.8	51	324	13.6	**62.2**
RoomSet2 ($T:100, k:100, \lambda:10^{-2}, c:5.2$)*										
10	F	11	11	0	100.0	100.0	10	22	31.3	90.9
11	F	13	11	1	91.7	84.6	9	16	36.0	69.2
12	M	8	8	2	80.0	100.0	8	20	28.6	100.0
13	F	10	8	2	80.0	80.0	10	92	9.8	100.0
14	F	10	7	3	70.0	70.0	10	20	33.3	100.0
Total		52	45	8	**84.9**	86.5	47	170	21.7	**90.4**

* Model parameters.

linear chain CRF algorithm that supports real-time inferencing proposed in [34] as opposed to the batch-inferencing version used previously in [21]. We present the *in-bed* and *out-bed* classification performance in Appendix C as our main focus is on bed-egress recognition. From these results (see Table V), we can observe that the proposed framework exhibits significantly lower number of FPs compared to our previous method, but the previous method depicts a higher number of TPs. We conclude that the proposed framework outperforms our previous method as there are lower number of FPs, and consequently, less false alarms.

When two room configurations are considered, we can see similar performance in terms of precision. However, *RoomSet1* depicts considerably lower recall compared to *RoomSet2*. Based on these observations, we can see that *RoomSet2* configuration performs better among the two room configurations.

We specifically investigated FPs and misses (i.e., number of missed bed-egress events, Actual $- TP$) in both room configurations. In the case of *RoomSet1*, there are 7 FPs and 42 misses. We identified that FPs are caused by sensor observations received from antenna A2 oriented toward the chair [see Fig. 2(b)]. These readings are from very weak signals—indicated by lower RSSI—and more likely to be due to reflections. These FPs can be addressed by reducing the RFID reader's receiver sensitivity on antenna ports; in this case, reducing the receiver sensitivity of A2's port. It is observed that all the misses are caused by insufficient sensor observations after a bed-egress. Out of 42, 24 misses have occurred in user trials that ended with a bed-egress and antenna A1, facing a standing person, failed to energize the W^{2}ISP and capture readings. Therefore, we further evaluated the *RoomSet1* bed-egress performance excluding the sensor data for the final 4 s for each trial. We believe this would better reflect real-world use of the proposed method where a person ambulating is likely to be recorded and classified albeit with a delay; these results are shown in Table VI. From these results we can see that the number of missed bed-egress for *RoomSet1* has reduced by 24, thereby increasing recall from 48.8% to 65.4%. Remaining misses can be mitigated by improving the W^{2}ISP design, particularly, improving power harvesting by improving the antenna design as indicated in [24] and using a hybrid-powered WISP, which is assisted by excess harvested power stored in a supercapacitor to prevent brownouts and improve reliability [39].

TABLE VI
BED-EGRESS RECOGNITION PERFORMANCE EXCLUDING FINAL 4 S FROM EACH TRIAL FOR *RoomSet1*

		Proposed Framework				BEAS Proposed in [21]			
Participant	Actual	TP	FP	Precision	Recall	TP	FP	Precision	Recall
1	6	5	0	100.0	83.3	4	39	9.3	66.7
2	4	3	2	60.0	75.0	4	14	22.2	100.0
3	4	1	1	50.0	25.0	3	6	33.3	75.0
4	3	3	0	100.0	100.0	3	2	60.0	100.0
5	5	5	0	100.0	100.0	4	7	36.4	80.0
6	9	6	1	85.7	66.7	6	78	7.1	66.7
7	6	5	1	83.3	83.3	6	48	11.1	100.0
8	5	1	1	50.0	20.0	3	116	2.5	60.0
9	10	5	1	83.3	50.0	6	14	30.0	60.0
Total	52	34	7	82.9	65.4	39	324	10.7	75.0

In contrast to *RoomSet1* deployment, which is designed to irradiate the entire room, *RoomSet2* deployment is designed to illuminate the areas where a patient is more likely to spend time, such as around the bed and the chair. In *RoomSet2* deployment, there are only eight FPs and seven misses. All the FPs have resulted when data is not available for $>$ 2-s period. In such an instance, the classifier incorrectly predicts an *out-bed*. When more sensor observations are available, the correct class label is predicted. The misses are also caused by the unavailability of sensor observations, particularly after a bed-egress.

B. Bed-Egress Movement Recognition Delays

Fig. 5 presents the distribution of bed-egress recognition delays for the proposed framework and the BEAS proposed in [21]. The vertical lines in Fig. 5 indicate the 90th percentile in respective distributions.

From Fig. 5, we can see that for the proposed framework $>$90% of the alarm instances are within the first 8 s for *RoomSet1* and within the first 6 s for *RoomSet2*. Generally *RoomSet2* performs better than *RoomSet1* as alarm delays are concentrated near zero, where there are virtually no delays. The main reason for this is the rich set of location information available from the RFID infrastructure in *RoomSet2* due to its configuration to monitor targeted areas.

Although there are higher FPs and lower TPs for BEAS, we can see that BEAS performs slightly better than the proposed framework in terms of delays. It is observed that, for BEAS, $>$90% of alarm instances are within the first 7 s for *RoomSet1*

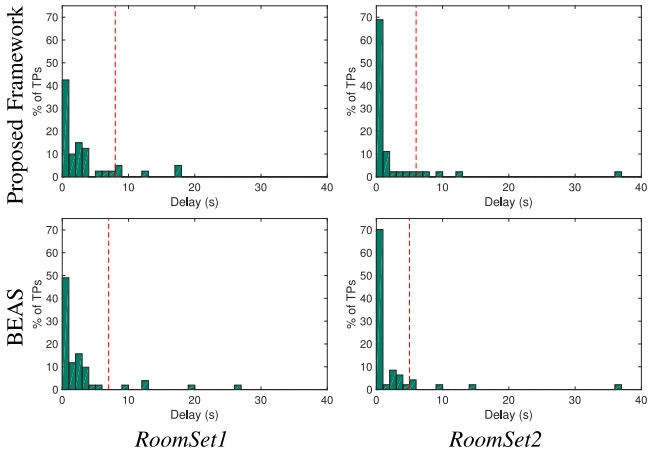

Fig. 5. Distribution of bed-egress movement recognition delays. Vertical lines indicate the 90th percentile of distributions.

TABLE VII
PERFORMANCE OF PREVIOUS BED-EGRESS MOVEMENT ALARMS

Bed-egress recognition approach	Precision	Recall	Participants' age (years)
Hilbe *et al.* [40]		96%	18-60
Bruyneel *et al.* [41]	100%	91%	37 ± 9 and 45 ± 11
Najafi *et al.* [8]*		93	66 ± 14
Godfrey *et al.* [12]*		83	77.2 ± 4.3
Proposed framework	85%	86%	66-86

* a sit-to-stand posture transition was considered as a bed-egress.

compared to 8 s and the first 5 s for *RoomSet2*, compared to 6 s for our proposed framework.

IV. DISCUSSION

We have proposed a framework to analyze bed-egress movements using a sparse acceleration and RFID data stream from a passive RFID sensor, i.e., W^{2}ISP. Specifically, based on motion analysis, we devised a novel sequence classification algorithm that is suitable for sparse data streams. Our framework not only relies on information from a triaxial accelerometer, but also considers information from the RFID infrastructure to successfully recognize bed-egress movements in real time while depicting a considerable performance improvement to that of our previously published method in [21].

Recently, several bed-egress movement sensor alarms have been reported in the literature. Most of these studies [8], [12], [40], [41] have been evaluated with healthy adult participants as opposed to older people. Hilbe *et al.* [40] and Bruyneel *et al.* [41] used pressure sensors attached to hospital beds. Najafi *et al.* [8] and Godfrey *et al.* [12] used wearable sensors strapped to participants for activity recognition and evaluated their approaches on data collected from older people, as in our study. Although movement sensor alarms were not the focus of these studies, they presented results for detecting sit-to-stand posture transitions that can be considered similar to a bed-egress movement. Table VII summarizes the results of previous bed-egress movement recognition approaches with the results obtained for *RoomSet2*. Although we cannot make a direct comparison with other studies because datasets and our experimental settings as well as sensors used are different, we can clearly see that the proposed framework performs comparably. Note that we have not considered specificity reported in previous studies since the activities considered as True Negatives could not be clearly established across the studies. Furthermore, our focus has been to evaluate precision and recall as motivated in Section II-G.

There are five major advantages arising from our approach.

1) The sensor design featuring a flexible antenna (predominately made from conductive fabric and foam) allows older people to move freely whilst wearing the device.
2) Unlike data from battery-powered accelerometers and gyroscopes [8], we use only noisy raw sensor data from a passive accelerometer and supplement this data with information from the RFID infrastructure to achieve performance comparable with existing approaches.
3) Our proposed framework for bed-egress recognition is highly responsive and reduces time delays to alarm so that caregivers are given a better opportunity to intervene while patients are undertaking unsupervised risky activities. In contrast, previous methods needed preprocessing of sensor data (such as filtering) [16] or a waiting time for sensors to reach a steady state ($\approx$ 2 min in [41]) prior to generating an alarm. Furthermore, approaches to handling activity label prediction inaccuracies in [8] and [42] rely on initiating notifications (i.e., alarms) after detecting a change in predictions (i.e., from *Sitting-on-bed* to *Standing*) and a subsequent *fixed evaluation* period (i.e., 10 s) to assess the consistency of the predicted activity label for subsequent sensor observations; this approach will incur a notification delay equal to the fixed evaluation period. Instead, we notify (e.g., alarm) at the *first instance of detecting a change in predictions* (e.g., from *sitting-on-bed* to *standing*). Our method requires no preprocessing as the novel sequence prediction algorithm accurately predicts bed-egress motion sequences using time-domain features.
4) Our batteryless sensor is low cost, can be disposed of if required and does not require maintenance (i.e., battery replacement or recharging). More importantly, it delivers promising results even when the sensor is attached over a loosely fitted hospital garment. Notably, Capezuti *et al.* [43] has shown that systems using bed sensors such as pressure mats needed daily maintenance to check the correct functionality, especially since they are subject to constant mechanical stress and are likely to move from their ideal placement on the bed. Moreover, pressure mats require disinfection or thorough cleaning because of possible exposure to body fluids, and protocols for controlling infections.
5) Although the proposed bed-egress sequence prediction algorithm is used to predict bed-egress motion sequences, it can be used in other sequence prediction problems having sparse data streams as in our case. However, the classification problem and data available from the data stream may require different features.

To realize these advantages, the RFID sensor platform does require an initial investment for the RFID infrastructure compared to battery-powered wireless sensors used in [15], [35],

and [42] . For instance, *RoomSet2* configuration cost is approximately 1200 USD, which is for a four-port RFID reader and three RFID antennas. In the RFID sensor platform, the cost is displaced from consumables (i.e., W^{2}ISP) toward infrastructure (i.e., RFID infrastructure). Since W^{2}ISP is inexpensive (3 USD per unit [21], [44]) and maintenance-free compared to battery-powered wireless sensors (≈300 USD per unit) employed in [15], [35], [42], a lower recurrent cost is expected. Unlike other wireless sensor deployments, the RFID infrastructure can also be used in other application scenarios such as patient tracking and hospital asset management.

Our study is not without limitations. First, the broadly scripted activity routines with the circumscribed duration (<2 h) of healthy older people using the sensor limited the number of tasks performed (25–27 per trial) in order to not over fatigue the participants. Second, as seen in Fig. 5, the responsiveness of the bed-egress recognition algorithm can, on occasions, be constrained by the time at which sensor observations can be acquired from the W^{2}ISP and potentially lead to an alarm delay. For example, an *out-bed* prediction may be after the physical transition of a patient because the W^{2}ISP was not adequately powered at the time of the patient transitioning out of bed. This can occur since the sensor must collect power from the antennas deployed in the room and this is a current limitation of the W^{2}ISP we have employed [23].

Further research to overcome present limitations should address the unavailability of sufficient sensor observations, especially during posture transitions by further developments in the wearable antenna elements used in the W^{2}ISP. In addition, investigating different sensor locations on the body and enhancements to the RFID reader antenna deployment, especially the more desirable layout in *RoomSet2*, should be investigated to enhance the sensor data collection. In order to confirm the performance of the system and acceptability of W^{2}ISP, future studies should consider a longitudinal monitoring study with unscripted activities. The study should include both day and night times and a population of hospitalized older patients in geriatric wards. It should be emphasized that, if caregivers were to respond to an alarm generated by our approach, as with existing alarm systems, there will always be a delay unless they are in the vicinity of the older person. Consequently, caregivers may not always be able to prevent a fall by intervening in time. Hence, the effectiveness of an alarm intervention in preventing a fall will also depend on the responsiveness of caregivers. However, this can be mitigated by concurrently implementing protocols to follow in responding to a bed-egress alarms and by using voice prompts to remind patients to seek supervisions prior to leaving the bed.

Appendix A Motion Recognition Using RSSI—Preliminaries

The RSSI indicates the power level of the backscattered tag response detected by the reader and this power is given by

$$\text{RSSI} = P_t G_t^2 G_{\text{path}}^2 K \tag{6}$$

where P_t is the output power of the reader, G_t is the gain of the reader antenna, K is the W^{2}ISP backscatter gain, and G_{path} is the one-way path gain of the deterministic multipath channel determined according to [23]

$$G_{\text{path}} = \left(\frac{\lambda}{4\pi d_0}\right)^2 \mid H \mid . \tag{7}$$

Here, d_0 is the direct path length and H is the channel response due to multipath. From (6) and (7), we can see that the RSSI is hypersensitive to distance d_0 as RSSI $\propto 1/(d_0)^4$. This indicates that the RSSI can be broadly used to approximate the distance between the sensor and a given antenna. As the distance between the W^{2}ISP and the distance to a given RFID antenna varies with activities, movements related to activities can be observed using RSSI.

Appendix B Features

A. Features from the Acceleration Sensor

We approximated the angles θ, α, and β as follows:

$$\theta \approx \tan^{-1}(a_f/\sqrt{a_v^2 + a_l^2}) \tag{8}$$

$$\alpha \approx \tan^{-1}(a_l/a_v) \tag{9}$$

$$\beta \approx \tan^{-1}(a_l/a_f). \tag{10}$$

Approximation of acceleration signals a_x, a_y, and a_z are as follows:

$$a_x \approx a_v \sin(\theta) + a_f \cos(\theta) \tag{11}$$

$$a_y \approx a_v \sin(\alpha) + a_l \cos(\alpha) \tag{12}$$

$$a_z \approx 1 + a_v \cos(\theta)\cos(\alpha) + a_l \sin(\alpha) + a_f \sin(\theta). \tag{13}$$

We approximated the change in velocity (Δv) and displacement (Δd) of the body motion on all three directions relative to the human body (anteroposterior axis-x; mediolateral axis-y; and dorsoventral axis-z) during a given subsequence according to (14). Here, we are interested in relative changes in velocity and displacement over a short duration of 2 s using raw acceleration values where ambient conditions do not change drastically and we can assume any drift in acceleration to be negligible.

$$\Delta v \approx \int_0^{\delta t} a\, dt \qquad \Delta d \approx \int_0^{\delta t} v\, dt. \tag{14}$$

For the calculation of change in resultant velocity Δv_r, we adopted the method presented in [12] where the authors have obtained the resultant acceleration a_r without considering gravity as follows:

$$a_r = \sqrt{a_f^2 + a_l^2 + a_v^2}. \tag{15}$$

B. Features from the RFID Platform

MI2 features were calculated as follows. First, MI matrix, M, was precalculated using training data sequences according to (5). Then, given a subsequence, $X_{[t_i-\delta t, t_i]}$, MI2(a) for antenna a is obtained as the weighted count of observations given by

$$\text{MI2}(a) = M_{a_i,a} \frac{1}{|X|} \sum_{j=1}^{|X|} \mathbf{1}_{[a_i = a_j]},\ a \in \mathcal{A}. \tag{16}$$

TABLE VIII
In-bed AND *Out-bed* LABEL PREDICTION PERFORMANCE

	RoomSet1		*RoomSet2*	
	Proposed	Baseline [21]	Proposed	Baseline [21]
Accuracy	94.0 ± 3.5	92.4 ± 3.8	96.1 ± 2.4	93.4 ± 5.2
Sensitivity	90.6 ± 8.1	84.5 ± 7.9	96.3 ± 6.3	74.2 ± 7.7
Specificity	94.7 ± 4.5	93.8 ± 3.5	96.2 ± 3.0	94.8 ± 3.9
G-mean	92.5 ± 4.1	89.0 ± 4.9	96.2 ± 3.3	83.7 ± 3.4

Here, a_i is the antenna ID of the ith sensor observation and j is the index of the sensor observation within the sequence X. It should be noted that the weights are obtained from M based on the antenna ID of the ith sensor observation, a_i, and the considered antenna a.

In the case of miC, we obtained value for each antenna combination $(a, a') \in \binom{A}{2}$ as

$$miC_{a,a'} = M_{a,a'} \,. \tag{17}$$

C. Features Based on a Label Sequence

We considered four features (ϕ_{pj}, $j = \{1 \ldots 4\}$) from previous labels $Y_{[t_i - \delta t, t_{(i-1)}]}$ and the current class label y.

Given the last three class labels, $Y_{\{i-3,i-1\}}$, feature ϕ_{p1} is calculated as

$$\phi_{p1} = \begin{cases} \{\mathbf{0}_3, Y_{\{i-3,i-1\}}\}; & \text{if } y = 1 \\ \{Y_{\{i-3,i-1\}}, \mathbf{0}_3\}; & \text{otherwise} \end{cases} \tag{18}$$

where $\mathbf{0}_3$ is a 1×3 zero vector and $\{.,.\}$ represents the concatenation of vectors.

For calculation of $\phi_{p2} \in R^2$ we considered class label sequence $Y' = \{Y_{[t_i - \delta t, t_{(i-1)}]}, y\}$. The value of the feature for the jth class $\phi_{p2}(j)$ is obtained as

$$\phi_{p2}(j) = \sum_{k=1}^{|Y'|} \mathbf{1}_{[Y'_k = j]} w_{t_k} \;, j = \{-1, 1\} \,. \tag{19}$$

Here, the weight w_{t_K} is as defined in the main text (see Section II-F).

For the calculation of $\phi_{p3} \in R^2$, we considered transitions: 1) *in-bed* to *out-bed*; and 2) *out-bed* to *in-bed*. Using the sequence of class labels $Y' = \{Y_{t_i - \delta t, t_{(i-1)}}, y\}$ we obtained number of transitions for jth transition $\phi_{p3}(j)$ as

$$\phi_{p3}(j) = \sum_{k=1}^{|Y'|-1} \mathbf{1}_{[j=(Y'_k, Y'_{k+1})]}, \; j = \{(-1,1), (1,-1)\} \,. \tag{20}$$

APPENDIX C SEQUENCE PREDICTION RESULTS

Here, we present the results for predicting *in-bed* and *out-bed* labels using the proposed sequence prediction algorithm. Table VIII lists the label prediction results for the proposed approach and the baseline approach [21] using both datasets (*RoomSet1* and *RoomSet2*). The baseline method uses three class labels, sitting-on-bed, laying-on-bed, and out-bed. Here, we compare the performance of predicting out-bed class label of the baseline approach with the proposed approach. From the results in Table VIII, we can see that the proposed method outperform the baseline method in all measures for both data sets. More importantly, the proposed sequential learning method showed statistically significantly higher ($p < 0.05$) performance in terms of sensitivity and G-mean measures for *RoomSet2*. Fig. 6 illustrates the normalized confusion matrices for the two datasets.

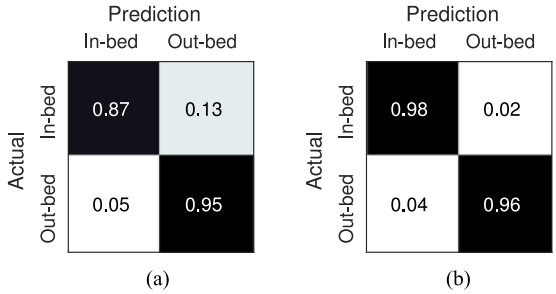

Fig. 6. Normalized confusion matrices for the proposed sequence learning algorithm.

ACKNOWLEDGMENT

The authors would like to thank Dr. S. Nair for helping to recruit volunteers for the trials and Mr. R.L. S. Torres for collecting the data used in this study. This study had ethics approval from the human research ethics committee of the Queen Elizabeth Hospital, South Australia (2011129).

REFERENCES

[1] K. D. Hill, M. Vu, and W. Walsh, "Falls in the acute hospital setting - impact on resource utilisation," *Aust. Health Rev.*, vol. 31, no. 3, pp. 471–477, 2007.
[2] National Patient Safety Agency, "The third report from the patient safety observatory: Slips, trips and falls in hospital," Tech. Rep. 0483, 2007.
[3] D. Oliver, F. Healey, and T. P. Haines, "Preventing falls and fall-related injuries in hospitals," *Clinics Geriatr. Med.*, vol. 26, no. 4, pp. 645–692, 2010.
[4] I. D. Cameron *et al.*, "Interventions for preventing falls in older people in nursing care facilities and hospitals," in *Cochrane Database of Systematic Reviews*. New York, NY, USA Wiley, 2010.
[5] C. A. Brand and V. Sundararajan, "A 10-year cohort study of the burden and risk of in-hospital falls and fractures using routinely collected hospital data," *Qual. Saf. Health Care*, vol. 19, no. 6, pp. e51–1–e51–7, 2010, doi:10.1136/qshc.2009.038273.
[6] Australian Commission on Safety and Quality in Health Care, *Preventing Falls and Harm From Falls in Older People: Best Practice Guidelines for Australian Community Care*. Sydney, Australia: Australian Commission on Safety and Quality in Health Care, 2009.
[7] N. Kosse, K. Brands, J. Bauer, T. Hortobagyi, and C. Lamoth, "Sensor technologies aiming at fall prevention in institutionalized old adults: A synthesis of current knowledge," *Int. J. Med. Inform.*, vol. 82, no. 9, pp. 743–752, 2013.
[8] B. Najafi, K. Aminian, A. Paraschiv-Ionescu, F. Loew, C. Bula, and P. Robert, "Ambulatory system for human motion analysis using a kinematic sensor: Monitoring of daily physical activity in the elderly," *IEEE Trans. Biomed. Eng.*, vol. 50, no. 6, pp. 711–723, Jun. 2003.
[9] L. Bao and S. S. Intille, "Activity recognition from user-annotated acceleration data," in *Pervasive Computing* (Lecture Notes in Computer Science). Berlin, Germany: Springer, 2004, no. 3001, pp. 1–17.
[10] D. Karantonis, M. Narayanan, M. Mathie, N. Lovell, and B. Celler, "Implementation of a real-time human movement classifier using a triaxial accelerometer for ambulatory monitoring," *IEEE Trans. Inf. Technol. Biomed.*, vol. 10, no. 1, pp. 156–167, Jan. 2006.

[11] M. Narayanan, S. Redmond, M. Scalzi, S. Lord, B. Celler, and N. Lovell, "Longitudinal falls-risk estimation using triaxial accelerometry," *IEEE Trans. Biomed. Eng.*, vol. 57, no. 3, pp. 534–541, Mar. 2010.
[12] A. Godfrey, A. Bourke, G. laighin, P. van de Ven, and J. Nelson, "Activity classification using a single chest mounted tri-axial accelerometer," *Med. Eng. Phys.*, vol. 33, no. 9, pp. 1127–1135, 2011.
[13] A. Henpraserttae, S. Thiemjarus, and S. Marukatat, "Accurate activity recognition using a mobile phone regardless of device orientation and location," in *Proc. Int. Conf. Body Sens. Netw.*, May 2011, pp. 41–46.
[14] S. Liu, R. Gao, D. John, J. Staudenmayer, and P. Freedson, "Multisensor data fusion for physical activity assessment," *IEEE Trans. Biomed. Eng.*, vol. 59, no. 3, pp. 687–696, Mar. 2012.
[15] K.-H. Wolf, K. Hetzer, H. M. z. Schwabedissen, B. Wiese, and M. Marschollek, "Development and pilot study of a bed-exit alarm based on a body-worn accelerometer," *Z. Gerontol. Geriatr.*, vol. 46, no. 8, pp. 727–733, 2013.
[16] D. C. Ranasinghe, R. L. Shinmoto Torres, K. Hill, and R. Visvanathan, "Low cost and batteryless sensor-enabled radio frequency identification tag based approaches to identify patient bed entry and exit posture transitions," *Gait Posture*, vol. 39, no. 1, pp. 118–123, 2014.
[17] N. Noury, A. Galay, J. Pasquier, and M. Ballussaud, "Preliminary investigation into the use of autonomous fall detectors," in *Proc. Int. Conf. IEEE Eng. Med. Biol. Soc.*, Aug. 2008, pp. 2828–2831.
[18] R. Steele, A. Lo, C. Secombe, and Y. K. Wong, "Elderly persons perception and acceptance of using wireless sensor networks to assist healthcare," *Int. J. Med. Inform.*, vol. 78, no. 12, pp. 788–801, 2009.
[19] G. Mountain *et al.*, "Developing and testing a telerehabilitation system for people following stroke: Issues of usability," *J. Eng. Des.*, vol. 21, no. 2–3, pp. 223–236, 2010.
[20] M. Gvercin *et al.*, "Defining the user requirements for wearable and optical fall prediction and fall detection devices for home use," *Inform. Health Soc. Care*, vol. 35, no. 3–4, pp. 177–187, 2010.
[21] R. L. Shinmoto Torres, D. C. Ranasinghe, Q. Shi, and A. P. Sample, "Sensor enabled wearable RFID technology for mitigating the risk of falls near beds," in *Proc. IEEE Int. Conf. RFID*, 2013, pp. 191–198.
[22] A. P. Sample, D. J. Yeager, P. S. Powledge, A. V. Mamishev, and J. R. Smith, "Design of an RFID-based battery-free programmable sensing platform," *IEEE Trans. Instrum. Meas.*, vol. 57, no. 11, pp. 2608–2615, 2008.
[23] D. C. Ranasinghe, Q. Z. Sheng, and S. Zeadally, *Unique Radio Innovation for the 21st Century: Building Scalable and Global RFID Networks*, 1st ed. New York, NY, USA: Springer, 2010.
[24] T. Kaufmann, D. C. Ranasinghe, M. Zhou, and C. Fumeaux, "Wearable quarter-wave folded microstrip antenna for passive UHF RFID applications," *Int. J. Antennas Propag.*, vol. 2013, pp. 129839-1–129839-11, 2013.
[25] EPCglobal Inc. (2015). EPC Radio-Frequency Identity Protocols Generation-2 UHF RFID. [Online]. Available: http://www.gs1.org/epcrfid/epc-rfid-uhf-air-interface-protocol/2-0-1
[26] Y. Su, A. Wickramasinghe, and D. C. Ranasinghe, "Investigating sensor data retrieval schemes for multi-sensor passive RFID Tags," in *Proc. IEEE Int. Conf. RFID*, San Diego, CA, USA, Apr. 2015, pp. 201–208.
[27] R. Sankarkumar, D. C. Ranasinghe, and T. Sathyan, "A highly accurate and scalable approach for addressing location uncertainty in asset tracking applications," in *Proc. IEEE Int. Conf. RFID*, Apr. 2014, pp. 39–46.
[28] S. Hariharan and S. T. S. Bukkapatnam, "Misplaced item search in a warehouse using an RFID-based partially observable Markov decision process (POMDP) model," in *Proc. IEEE Int. Conf. Autom. Sci. Eng.*, Aug. 2009, pp. 443–448.
[29] C. Sutton and A. McCallum. (Nov. 2010). "An introduction to conditional random fields," [Online]. Available: http://arxiv.org/abs/1011.4088
[30] A. Bordes, N. Usunier, and L. Bottou, "Sequence labelling SVMs trained in one pass," in *Machine Learning and Knowledge Discovery in Databases* (Lecture Notes in Computer Science). Berlin, Germany: Springer, Jan. 2008, no. 5211, pp. 146–161.
[31] I. Tsochantaridis, T. Joachims, T. Hofmann, and Y. Altun, "Large margin methods for structured and interdependent output variables," *J. Mach. Learn. Res.*, pp. 1453–1484, 2005.
[32] S. Shalev-Shwartz, Y. Singer, N. Srebro, and A. Cotter, "Pegasos: Primal estimated sub-gradient solver for SVM," *Math. Program.*, vol. 127, no. 1, pp. 3–30, 2011.
[33] A. Wickramasinghe and D. C. Ranasinghe, "Recognising activities in real time using body worn passive sensors with sparse data streams: To interpolate or not io interpolate?" presented at the Int. Conf. Mobile and Ubiquitous Systems: Computing, Networking and Services, Coimbra, Portugal, Jul. 2015.
[34] R. L. Shinmoto Torres, D. C. Ranasinghe, and Q. Shi, "Evaluation of wearable sensor tag data segmentation approaches for real time activity classification in elderly," in *Proc. Int. Conf. Mobile and Ubiquitous Syst.: Comput., Netw. Serv.*, Tokyo, Japan, 2013, pp. 384–395.
[35] J. P. Varkey, D. Pompili, and T. A. Walls, "Human motion recognition using a wireless sensor-based wearable system," *Pers. Ubiquitous Comput.*, vol. 16, no. 7, pp. 897–910, 2012.
[36] L. Wang, T. Gu, H. Xie, X. Tao, J. Lu, and Y. Huang, "A wearable RFID system for real-time activity recognition using radio patterns," in *Mobile and Ubiquitous Systems: Computing, Networking, and Services*. Berlin, Germany: Springer, 2013.
[37] M. Sokolova and G. Lapalme, "A systematic analysis of performance measures for classification tasks," *Inform. Process. Manage.*, vol. 45, no. 4, pp. 427–437, Jul. 2009.
[38] M. Kubat, R. Holte, and S. Matwin, "Learning when negative examples abound," in *Machine Learning* (Lecture Notes in Computer Science). Berlin, Germany: Springer, 1997, pp. 146–153.
[39] Y. Dong, A. Wickramasinghe, H. Xue, S. Al-Sarawi, and D. C. Ranasinghe, "A Novel Hybrid Powered RFID Sensor Tag," in *Proc. IEEE Int. Conf. RFID*, San Diego, CA, USA, Apr. 2015, pp. 55–62.
[40] J. Hilbe, E. Schulc, B. Linder, and C. Them, "Development and alarm threshold evaluation of a side rail integrated sensor technology for the prevention of falls," *Int. J. Med. Inf.*, vol. 79, no. 3, pp. 173–180, 2010.
[41] M. Bruyneel, W. Libert, and V. Ninane, "Detection of bed-exit events using a new wireless bed monitoring assistance," *Int. J. Med. Inform.*, vol. 80, no. 2, pp. 127–132, 2011.
[42] F. Bianchi, S. Redmond, M. Narayanan, S. Cerutti, and N. Lovell, "Barometric pressure and triaxial accelerometry-based falls event detection," *IEEE Trans. Neural Syst. Rehabil. Eng.*, vol. 18, no. 6, pp. 619 –627, Dec. 2010.
[43] E. Capezuti, B. L. Brush, S. Lane, H. U. Rabinowitz, and M. Secic, "Bed-exit alarm effectiveness," *Arch. Gerontol. Geriatr.*, vol. 49, no. 1, pp. 27–31, 2009.
[44] M. Buettner, R. Prasad, M. Philipose, and D. Wetherall, "Recognizing daily activities with RFID-based sensors," in *Proc. Int. Conf. Ubiquitous Comput.*, 2009, pp. 51–60.

Asanga Wickramasinghe (S'03–M'01) received the B.Sc. degree in information and communication technology from the University of Colombo School of Computing, Colombo, Sri Lanka, in 2010. He is currently working towards the Ph.D. degree at the School of Computer Science, University of Adelaide, Adelaide, Australia.

His main research interests include machine learning, data mining, pervasive computing, and software engineering.

Damith C. Ranasinghe (S'03–M'12) received the Ph.D. degree in electrical and electronic engineering from the University of Adelaide, Adelaide, Australia, in 2007 under P. H. Cole and B. R. Davis.

During his Ph.D., he held an internship position at the Massachusetts Institute of Technology (MIT), Cambridge, MA, USA, in 2004, and from 2005 to 2006, he was a Research Engineer at the then Auto-ID Center founded at MIT. Since 2007, he has been a Postdoctoral Researcher at the University of Cambridge, Cambridge, U.K., from 2007 to 2009. He joined the University of Adelaide in 2010 and is currently a tenured Senior Lecturer at the School of Computer Science where he leads the research group at the Adelaide Auto-ID Lab. His research interests include pervasive computing, wearable computing, human activity recognition, gerontechnology, and lightweight cryptography for resource constrained devices.

Christophe Fumeaux (M'03–SM'09) received the Diploma and Ph.D. degrees in physics from the ETH Zurich, Zürich, Switzerland, in 1992 and 1997, respectively.

From 1998 to 2000, he was a Postdoctoral Researcher at the University of Central Florida, Orlando, FL, USA. In 2000, he joined the Swiss Federal Office of Metrology, Bern, Switzerland, as a Scientific Staff Member. From 2001 to 2008, he was a Research Associate with the Laboratory for Electromagnetic Fields and Microwave Electronics, ETH Zurich. Since 2008, he has been with The University of Adelaide, Adelaide, Australia, where he is currently a Professor with the School of Electrical and Electronic Engineering. His current main research interests include computational electromagnetics, antenna engineering, terahertz technology and the application of RF design principles to optical micro/nanostructures.

Prof. Fumeaux has served as an Associate Editor for the IEEE TRANSACTIONS ON MICROWAVE THEORY AND TECHNIQUES from 2010 to 2013. Since 2013, he has been serving as a Senior Associate Editor, and since 2015, as an Associate Editor-in-Chief for the IEEE TRANSACTIONS ON ANTENNAS AND PROPAGATION. He received the ETH Silver Medal of Excellence for his doctoral dissertation. From 2011 to 2015, he was a Future Fellow of the Australian Research Council. He received/coreceived best journal paper awards, including the 2004 ACES Journal and 2014 IEEE Sensors Journal, as well as best conference paper awards at the 2012 Asia-Pacific International Symposium on Electromagnetic Compatibility and the 17th Colloque International sur la Compatibilité Electromagnétique.

Keith D. Hill received the Ph.D. degree investigating balance dysfunction and falls risk in older people from The University of Melbourne, Parkville, Australia, in 1998.

He is a physiotherapist, graduating with a BAppSc Physio from Lincoln Institute of Health Sciences, in 1980. He is currently the Head of the School of Physiotherapy and Exercise Science, Curtin University, Perth, Australia, and his main research interests include ageing, rehabilitation, exercise, and falls prevention across community, hospital, and residential care settings.

Renuka Visvanathan (PhD, FRACP, MBBS) is a specialist Geriatrician who is the Director of Aged Extended Care Services, Queen Elizabeth Hospital, Central Adelaide Local Health Network, Woodville South, Australia. She is also Professor of geriatric medicine with the Adelaide Geriatrics Training and Research with Aged Care Centre, University of Adelaide, Adelaide, Australia. Her research interests include clinical syndromes in older people and this includes frailty, undernutrition, falls and dementia.